INTERNATIONAL JOURNAL OF RESEARCH – GRANTHAALAYAH
A knowledge Repository

Science

DERIVATION OF LAND SURFACE TEMPERATURE (LST) FROM LANDSAT 7 & 8 IMAGERIES AND ITS RELATIONSHIP WITH TWO VEGETATION INDICES (NDVI AND GNDVI)

Richard J. U. [1], Ibochi Andrew Abah [2]
[1] Department of Special Survey, Office of the Surveyor General, Moscow Road, Port Harcourt, Nigeria
[2] Department of Surveying & Geoinformatics Federal Polytechnic, Bauchi, Nigeria.

Abstract

Land surface temperature (LST) fluctuation is a global problem that is responsible for regional and global climate change. Abnormal LST causes drought, depletion of ozone layers, skin and lung diseases and also affect crops production. Spatial distribution of surface temperature has become an issue especially to less developed countries with little or absent of temperature stations to report daily or monthly temperature of the area. This study utilized remote sensing approach to estimate land surface temperature, NDVI and GNDVI of Port Harcourt, Rivers State, Nigeria. The study was conducted using Landsat imageries of two epochs (1990 and 2017) which was downloaded using path 188 and row 57. The images were converted from DN to TOA radiance using algorithm specified in the Landsat user's guide. The highest estimated LST in 1990 and 2017 map was 28.77°C and 29.37°C. Also, in 1990 the highest LST was recorded in Diobu and part of Old Port Harcourt Township while in 2017 maximum temperature extended from Diobu to Trans-amadi. The increase LST was due to urbanization and industrialization in the city. The study observed mean difference between estimated LST of 1990 and 2017 and that observed by NIMET as 1.24°C and 2.91°C respectively. There was positive correlation coefficient of 0.09 and 0.4 between LST against NDVI in 1990 and in 2017 and between LST against GNDVI of 0.19 and 0.30 was also observed in both years. This study justified that remote sensing and GIS can be used to derive LST which can be used for environmental studies and research purposes. For further study, LST should be estimated in all the state and their values validate with in-situ observations.

Keywords: GNDVI; Land Surface Temperature; Isotherm Map; NDVI; OLI Landsat 8; Remote Sensing; TOA Radiance.

1. Introduction

Land surface temperature (LST) is defined as the temperature at a particular location on the earth's surface [1]. It is synonymous with global temperature (GT), sea surface temperature (SST), and land surface air temperature (LSAT) [2]. The estimation of surface temperature has been extended from the in-situ-based observations to the remote sensing-based methods. The remote sensing method of estimating surface temperature has the following advantages; large area coverage, ability to estimate temperature in accessible areas, very efficient and effective method, and above all, is cost effective. Remote sensing has been used in the field of meteorology and climatology in the estimation of surface temperature [3]; [4].

The estimation of LST over the earth's surface is very important for the understanding of the relationship between biotic and abiotic components of the environment. LST has direct impacts on crop productivity [5]; [6]; [7]. Surface temperature affects ground water quality [8], groundwater temperature [9]; [10]. Of great concern globally is the problem of climate change due to temperature fluctuations [11]; [12]. Climate change has affected crops productivity [13], causes severe urban flooding [14]; [15]; [16]. Global temperature fluctuations started since 1850 due to accumulation of greenhouse gases (CO_2, N_2O, and CH_4) in the atmosphere [17]. The main driver of greenhouse gas in the atmosphere is CO_2 [18].

Land surface temperature is directly related to vegetation indices (VIs). VI is aimed at displaying and inventorying image pixel with green vegetation [19]. Vegetation indices are useful in forest management for the determination of the presence of green vegetation, health and vegetation abundance. Green vegetation cover has very distinctive interactions with the energy in the visible (band 1-3) and near-infrared region of the electromagnetic spectrum from satellite sensor. Hence, the development of several algorithms to computes the interactions between green vegetation and electromagnetic spectrum in the field of remote sensing. The algorithms for computing VIs were first developed in the 1970s for assessing vegetation health [20]. Some of these vegetation indices are used in the estimation of urban heat island and urban microclimate studies [21].

Several datasets have been used by many researchers to estimate surface temperature and compare the relationship with VIs using regression analysis in many urban areas. Landsat and AVHRR data were used to estimate surface temperature from 1986 – 1996 in the central coast of Maine [22]. [23] used Landsat data to derived surface temperature and compared the results with NDVI. Similarly, [24], [25]) used split-window algorithm to estimate surface temperature from AHVRR image and compare the relationship with in-situ temperature. In the study area, there were no spatially distributed temperature stations that will report at least monthly LST at selected locations, except the only station in Port Harcourt international airport Omagwa that only reported one LST for the entire city. This situation has been a concern to many researchers, especially, in the environmental management. This study utilized Landsat imagery of 1990 and 2017 to derive LST and the vegetation indices (namely; NDVI and GNDVI) and compute the correlation coefficient using sample points of LST and vegetation indices values.

1.1. Study Area

Port Harcourt Local Government Area, Rivers State, Nigeria is situated on 286867mE – 273040mE and 533530mN – 521228mN in WGS84, Zone 32N. It has an approximate area of

11048.9ha, covered by different land use/ land cover with a total population of 541,115 people [26]. Available land use/ land cover in the area include; (a) water body (b) Built-up areas (c) Mangrove vegetation along rivers and creeks shorelines (d) Vegetation and wetland. The mean temperature ranges between 30.0°C - 33.0°C and annual rainfall ranges between 2100 mm – 4600mm [27]. The study area is without spatially distributed temperature stations except the only station in Port Harcourt International Airport Omagwa. It was selected because (a) there was no spatially distributed temperature stations that can provide researchers, professionals and government agencies with temperature data (b) of the abnormal temperature observed in the city in 2017 and in the first quarter of 2018, resulting in urban flooding in 2017 [28]. This study evaluates the trend of land surface temperature in the city between 1990 and 2017 using Landsat satellite imageries. Figure 1 is the map of the study area produced from ESRI's ArcGIS 10.1 software.
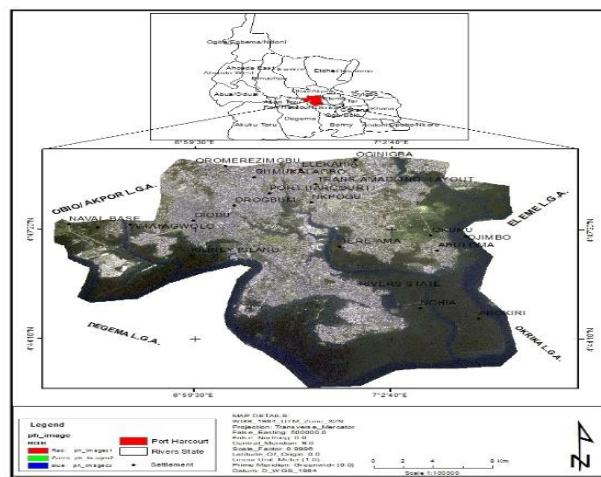
Figure 1: Map of the study area produced from SPOT imagery.

2. Materials and Software

The software used in this study is ESRI's ArcGIS 10.1: The software strength is in vector data processing. It was used to perform image clipping, conversion of DN to TOA radiance, estimation of LST, derivation of vegetation indices and for the compilations of maps. ArcGIS software was selected because it contained tool for raster calculations and produce satisfactory results. LST can also be derived using Environment for Visualizing Images (ENVI) software [29] and PANCROMA[TM] [30]. PANCROMA[TM] can be purchase at subsidized rate from the web link www.PANCROMA.com.

The estimation of land surface temperature was carried out using Landsat imageries of two epochs. The Landsat imageries were downloaded from its website (http://glovis.usgs.gov/) using path 188 and row 57 in zip file format which also contained the header file. The Landsat imageries selected for download was the precision orth-corrected product (LIT) that has been corrected for radiometric and geometric distortions [31]. The image was acquired in GMT which was converted to local time and Nigeria is one hour ahead of GMT. The processing was based on the local time of Nigeria. In addition, shape file of Port Harcourt used to clip the extent of the study area and the settlement shape file was obtained from OSGRV on application. Table 1 shows the characteristics of the Landsat data used in the derivation of land surface temperature and vegetation indices.

Table 1: Properties of Landsat satellite image used for the study.

Sensor	Acqui. Date	Acqui. Time	Band and Range (µm)	Resolution (m)
Landsat TM	12/22/1990	10: 04: 09	B2= GREEN = 0.52 – 0.60	30 x 30
			B3= RED = 0.63 – 0.69	,,
			B4= NIR = 0.76 – 0.90	,,
			B6= TIR= 10.40 – 12.50	Resample
Landsat OLI	1/6/2017	10: 45: 23	B3= GREEN= 0.53 – 0.59	30 x 30
			B4= RED= 0.64 – 0.67	,,
			B5= NIR= 0.85 – 0.88	,,
			B10= TIR-1= 10.60 – 11.19	Resample

2.1. Data Processing

The shape file of Port Harcourt Local Government Area was used to clip Landsat satellite imageries band by band in ESRI's ArcGIS 10.1. Image clipping using shape file defines the extent of the area [32]. Clipping operations were performed from the raster processing tools in data management of the Arc Toolbox. The Landsat band selected for the 1990 image are band 2, 3, 4, 6, while for the 2017 image, the bands selected are band 3, 4, 5 and 10 respectively. These bands were selected because band 3 is used in distinguishing vegetation from soil while band 6 is the thermal band for Landsat TM [33] and also band 10 is the thermal band for Landsat OLI [34]. Band 2, 3 and 4 for TM and band 3, 4, and 5 for OLI images have 30m x 30m spatial resolutions. Accordingly, band 6 of TM has 120m x 120m spatial resolution [35]; [36] while band 10 of OLI image has 100m x 100m resolution [34]. But these bands (band 6 and 10) were resampled to 30m x 30m resolution by the data provider prior to the data download. This has not only enhanced processing speed but also allows uniformity in the data during analysis, especially, the sampling of LST and VIs values from the maps on pixel base. Generally, Landsat data have been geo refenced to WRS-1 & 2 during processing at the base station. The WRS-2 was used to reference all Landsat OLI, TM and ETM+ [34]; [37]. This study was based on these referenced images. The images were radiometrically corrected by the data provider. However, before computing surface temperature, the images were converted from digital number (digital count or gray value) to Top of atmosphere (TOA) radiance which represents the actual reflectance from the earth's surface. The DN is a dimensionless unit and does not represent any physical quantity [38], hence, the need for its conversion. The conversion and computation of surface temperature follows the formulae quoted in the Landsat user's guide.

For Landsat OLI, TOA radiance is computed using the formula

$$L_\lambda = M_L \times Q_{cal} + A_L \text{ -- 1}$$

Where, L_λ is the spectral radiance in $Wm^{-2}Sr^{-1}$, M_L is the radiance multiplicative scaling factor for the band, Q_{cal} is the L1 pixel value in DN and A_L is the radiance additive scaling factor for the band [34].

The surface temperature was computed from the TOA radiance image using the formula,

$$T = K2/ In (K1/ L_\lambda + 1) \text{ -- 2}$$

Where, T is the TOA brightness temperature in Kelvin, L_λ is the spectral radiance in $Wm^{-2}Sr^{-1}$, K1 and K2 are the thermal constant for band 10. The parameters M_L, A_L, K1, and K2 are obtained from the Landsat header file.

Similarly, for Landsat TM, TOA radiance in $Wm^{-2}Sr^{-1}$, was computed using the formula,

$L_\lambda = (LMAX_\lambda - LMIN_\lambda)/ QCALMAX - QCALMIN \times (DN - QCALMIN) + LMIN_\lambda$ ------------ 3

Where, $LMAX_\lambda$, and $LMIN_\lambda$ are the maximum and minimum spectral radiance for the band, QCALMAX and QCALMIN are the maximum and minimum quantize calculated for the band, and DN is the pixel DN value [38].

While the surface temperature from the computed radiance is given by,

$T = K2/ In(K1/ L_\lambda + 1)$ -- 4

Where, T is the TOA brightness temperature in Kelvin, L_λ is the spectral radiance in $Wm^{-2}Sr^{-1}$, K1 and K2 are the thermal constant for band 6. For Landsat TM, the value of K1 and K2 are 607.74K and 1260.56K respectively. The computed temperature in Kelvin scale was converted to Celsius scale using the relationship,

$C = T - 273.15$ -- 5

Where, T is the Kelvin temperature, and C is the Celsius temperature. The value 273.15°C is the absolute zero temperature for converting Kelvin scale to Celsius scale. This conversion was necessary in other to compare in-situ land surface temperature broadcast by NIMET on daily basis to the satellite derived values. The temperature maps in Celsius were reclassified into five classes of equal interval ranging from very low temperature to very high temperature.

Similarly, the Celsius temperature values was extracted using sample tool as points in x, y, z (where x and y is the easting and northing coordinate and z is the Celsius temperature of that point) from each pixel and was used to plot isotherm map of the area. Isotherm is a map showing locations of equal surface temperature represented by smooth spline lines. Isotherm map was produced using 3D Analyst Tools from ArcGIS 10.1 software. [39] Produced isotherm map of Ahmedabad city India from QGIS. A total of 122,772 points (x, y, and z) was extracted from the LST maps (1990 and 2017 map) and was used to generate isotherm maps for the two years.

Vegetation Indices: Two vegetation indices were computed from the Landsat imageries and their values correlated with the estimated surface temperature map. Normalized difference vegetation index (NDVI) and green normalized difference vegetation index (GNDVI) were selected due to their ability in representing green and health of vegetation. NDVI was first proposed by Reuse et al, 1974 [40] and is computed according to [35] by the equation,
NDVI = (Near infrared – Red)/ (Near infrared + Red) -- 6

For OLI data, near infrared band is the band 5 and red band is the band 4. Similarly, for the TM, near infrared is the band 4 and red band is the band 3. These bands were carefully selected in the map algebra.

The values of NDVI map ranges from -1 to 1 which indicates the variations of green and healthy vegetation type in the given area. The higher the NDVI value the denser the vegetation and the lower the NDVI the less dense or absent of vegetation cover.

Similarly, GNDVI is given by the equation,

GNDVI = (Near infrared – Green)/ (Near infrared + Green)   --- 7

Where, near infrared is the band 4 for TM and band 5 for OLI data and green band is the band 2 and band 3 for Landsat TM and OLI data respectively.

GNDVI is a modification of NDVI by replacing red band with green band in the equation of NDVI.

Correlation Analysis: Correlation analysis provides a means of measuring the strength of relationship between variables (dependent and independent) that are quantitative, in this case, surface temperature as dependent and VIs indices as independent variables. This relationship is tested using correlation coefficient (r) which provides standardized measure of linear association between variables [41]. The degree of the relationship ranges from -1 (indicating perfect negative correlation) to +1 (indicating perfect positive correlation) between variables [42]. Correlation analysis may be computed using SPPS, excel spread sheet, IDRISI software etc. The surface temperature for the two epochs was sample at 30m grid interval (corresponding to raster grid cell) in the spatial analyst tools into excel spreadsheets. Similarly, the VIs values were extracted and merge with the estimated surface temperature for the correlation analysis to be performed. A total of 122,772 points (x, y, and z) was sampled from the LST maps (1990 and 2017 map) and the vegetation indices covering the entire area into excel spread sheet. In this analysis, estimated surface temperature was chosen as dependent (y-axis) variable while VIs (NDVI or GNDVI) was taken as independent (x-axis) variable. The correlation coefficient (r) was given by the model,

$$r = \sum(x - \bar{x})(y - \bar{y})/(n - 1)SxSy$$ -- 8

Where, x is the independent variable, y is the dependent variable, n is the number of sample, Sx and Sy are the sample standard deviation of measured variable x and y [41].

3. Results and Discussion

The estimated surface temperature map of the study area was shown in figure 2a and 2b for the two epochs (1990 and 2017). The derived surface temperature for the two years was assigned equal class and colour and the temperature calculated in Celsius degrees. Figure 2a is the estimated surface temperature in 1990 with the very low values in the range 17.90°C – 20.10°C. The very low temperature areas occurs at two isolated locations with one location in Tere-Ama water body adjourning wetland and another location in the river south of Borokiri in the Old Port Harcourt Township. Very low surface temperature areas were represented on the map in Cretan blue colour.

The very low temperature was followed by low temperature region ranging from 20.10°C – 22.27°C. It was represented by Fuchsia pink colour and predominantly located partly in the mangrove vegetation, shoreline and water body. It is mostly located in the south and followed the water channel to the northern part of the city. The moderately high surface temperature values ranges from 22.27°C – 24.43°C, represented by Cantaloupe colour located in the light vegetation and mangrove vegetation in the east of Eagle Island, south of Abuloma, east of Amadi-ama road towards Dr Peter Odili road and in the fringes of built-up and mangrove swamp in the southern part of Borokiri. It is the largest land use/ land cover with this temperature range. The high land surface temperature zones which was represented on the map with Ginger pink ranges from 24.43°C – 26.60°C. These regions are located within buffer zones of densely built-up and less dense built-up areas, for example, Eagle Island, Old G.R.A, Orogbum, part of Elekahia, and Oginigba slaughter areas. Very high land surface temperature zones with values ranging from 26.60°C – 28.77°C was shown on the map with Mar red colour. These zones are located in the densely built-up areas like Diobu, from Station Road to Kolokuma Street in the Old Port Harcourt Township, a location in Azubie and three locations in Abuloma including a location in Okilo Street.

Similarly, for the 2017 estimated surface temperature as shown in figure 2b, the very low surface temperature ranges from 20.38°C – 22.18°C. It was represented by Cretan blue and was found in eighteen locations south of Borokiri and five locations east of Eagle Island, mostly in the water body. Low land surface temperature ranges from 22.18°C – 23.97°C was located in the mangrove and wetlands of Borokiri and Eagle Island and transited the water course of the area to the wetland of Ogbunabali and Nkpogu. It was represented on the map by Fushia pink colour. The moderately high surface temperature with values ranges from 23.97 – 25.77°C as represented by Cantaloupe was located in the riparian vegetation which is the boundary of built-up and the swamp. It is a zone of moderate temperature. The high surface temperature zones with values ranges from 25.77°C – 27.57 °C was represented on the map by Ginger pink. These zones are located within the built-up areas, mostly in the settlements along water source with moderate land surface temperature, such areas are; Eagle Island, RSU and the adjourning streets in Diobu near river bank, Old G.R.A., Borokiri, Nkpogu, Tere-ama and Abuloma. The last zone was the very high surface temperature values ranges from 27.57°C – 29.37°C. It is the hottest zones on the map and was shaded with Mar red colour. These zones are found in Diobu, Orogbum, Rumuokalagbor, Elekahia, Slaughter, Trans-amadi, Azubie, five isolated locations in Old Port Harcourt Township and three locations in Abuloma.
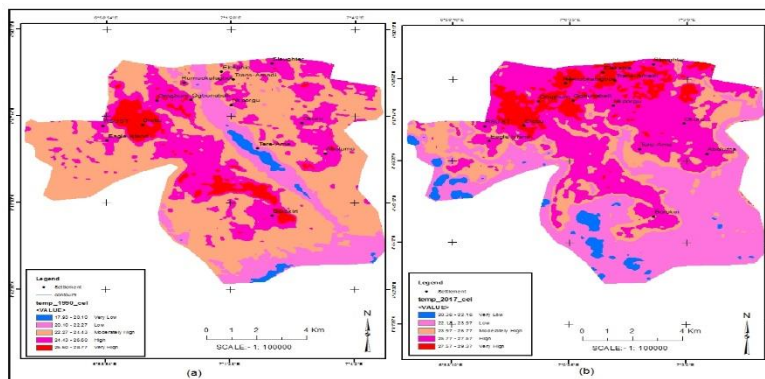
Figure 2: Estimated land surface temperature (LST) map, (2a) LST in 1990 left and (2b) LST in 2017 right.

Table 2 shows the minimum, maximum and mean surface temperatures on 1/6/1990 and on the 12/22/2017 obtained from Landsat satellite image. The derived mean temperature was compared with the in-situ measurement obtained from NIMET. The mean estimated LST in 1990 was 23.74°C while the NIMET reported in the same month with the estimated was 22.50°C. Similarly in 2017 the mean LST was 25.08°C and NIMET broadcast was 27.99°C in same month.

Table 2: The comparison of estimated land surface temperature and the in-situ temperature observe by NIMET for the 1990 and 2017.

Satellite	Estimated lst			Nimet lst (°c)		
	Min. Lst (°c)	Max. Lst (°c)	Mean lst (°c)	Min.	Mean	Max.
Landsat 1990	17.93	28.77	23.74	22.40	22.50	24.40
Landsat 2017	20.38	29.37	25.08	22.20	27.99	23.64

Figure 3a – b was the isotherm map of 1990 and 2017 produced from the sample points over the LST map. The isotherm was produced using ArcGIS 10.1 software and brown colour was chosen to represents LST location on the earth as in the case of contour line. Since the temperature range in 1990 was 10.84°C and that of 2017 was 8. 99°C, the isotherm was plotted from the 3D Analyst Tools at an interval of one (1) degree Celsius.
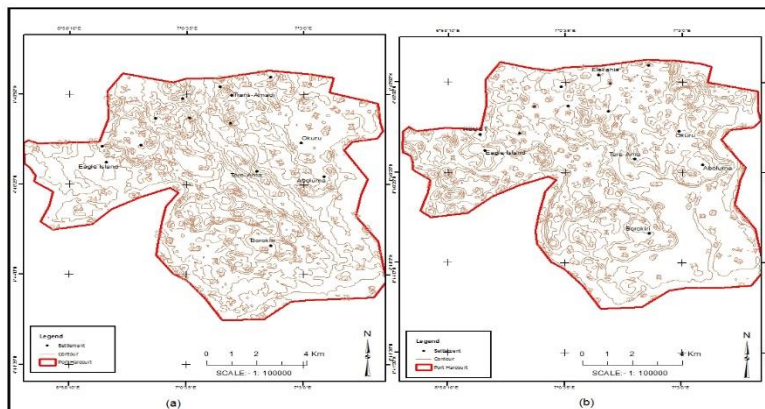
Figure 3: Derived isotherm for the area, (3a) isotherm in 1990 left and (2b) isotherm in 2017 right.

Figure 4a and 4b was the NDVI map of 1990 and 2017 of the study area. In 1990 map, the very low green vegetation ranges from -0.30 - -0.13 located in the water body. The values indicate absence of vegetation in the water body. The second class is the low vegetation zones ranges from -0.13 – 0.04 located on the map within the built-up areas. The moderately high zones ranges from 0.04 – 0.22 and was found along the water course and wetland. The high vegetation zones ranges from 0.22 – 0.39 located in the mangrove vegetation and light vegetation within built-up areas. Finally, the very high vegetation with NDVI values ranges from 0.39 – 0.56 indicated the presence of healthy vegetation. They are located in the eastern part of Eagle Island, Okuru and some isolated areas in the north of Orogbum.

For the 2017 NDVI map in figure 4b, the values of NDVI changes dramatically with the very low values ranges from -0.28 - -0.20 and these zones cover the water body and part of the wetland in

the south of Borokiri. The very high NDVI values ranges from 0.03 - 0.11 in an isolated areas on the map, mostly south of Eagle Island and Borokiri. It indicates the presence of scanty vegetation.
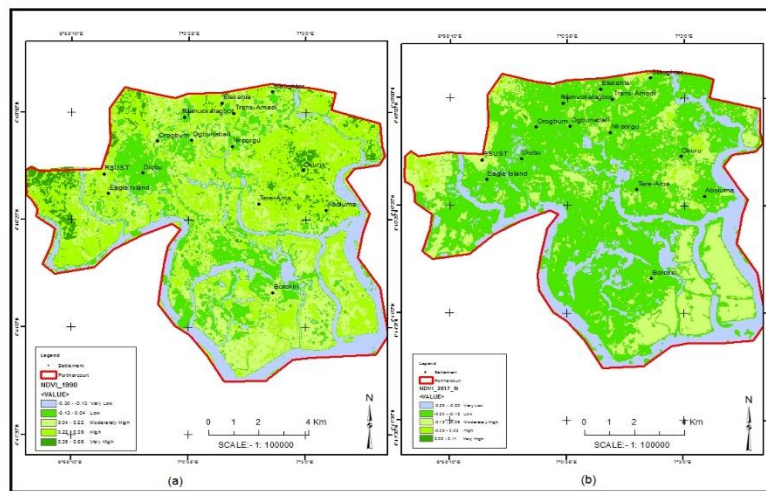
Figure 4: Derived NDVI map, (4a) NDVI in 1990 left and (4b) NDVI in 2017 right.

Figure 5a – b presented the results of GNDVI of 1990 and 2017 map respectively. In figure 5a the GNDVI of 1990 map shows very low green vegetation areas with values ranges from -0.49 - -0.49, mostly in the water body. The values indicated absence of green vegetation in those areas. Also the very high green vegetation was observed in the western part of Eagle Island, Okuru, and partly in the northern part of Orogbum. It ranges from 0.22 – 0.39 as shown on the GNDVI map of 1990. Similarly, for the GNDVI of 2017 map, the very low green zones ranges from -0.41 - -0.34 and was located in the water body. These zones was followed by the low green ranges from -0.34 - -0.26 as shown with Quetzal green colour. The very high green zones ranges from -0.11 – -0.0 which was located in some isolated areas in the east of Eagle Island.
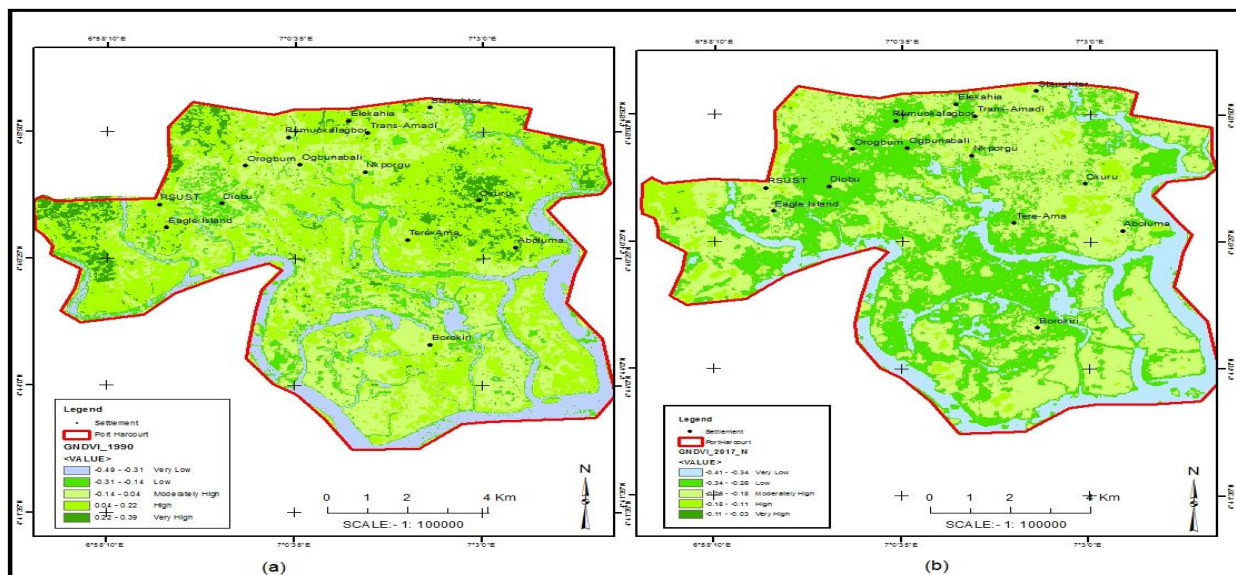
Figure 5: Derived GNDVI map, (5a) GNDVI in 1990 left and (5b) GNDVI in 2017 right.

Table 3 summarizes the computed NDVI and GNDVI for the 1990 and 2017 maps. In 1990 map, the calculated NDVI minimum and maximum values are -0.30 and 0.56 respectively, while the computed minimum and maximum values of GNDVI are -0.49 and 0.39 respectively. Similarly, the calculated minimum and maximum NDVI values for the 2017 map are -0.16 and -0.03 respectively. The Pearson coefficient of correlation (r) between LST against NDVI in 1990 sample points was 0.09 and that of LST versus NDVI in 2017 data was 0.40.

Table 3: Result of correlation analysis of 1990 and 2017 of LST against NDVI and GNDVI.

IMAGE	NDVI	GNDVI	r = LST VS NDVI	r= LST VS GNDVI
Landsat 1990	MIN. = -0.30 MAX. = 0.56 MEAN = 0.13	MIN. = -0.49 MAX. = 0.39 MEAN = -0.01	0.09	0.19
Landsat 2017	MIN. = -0.28 MAX. = 0.11 MEAN = -0.16	MIN. = -0.41 MAX. = -0.03 MEAN = -0.27	0.40	0.30

3.1. Discussion

Land surface temperature for the two epochs corresponds to the land use/ land cover of the area. In 1990, the urban temperature was highest in the built-up areas with mean temperature of 27.69°C. But in 2017 map, LST extended in area to the north and east of the city. This increase may be due to combine temperature from solar radiation and those radiated from the man-made structures like road, building, and those from industrial and residential areas [43]. The land surface temperature corresponds to the city growth, that is, as the city expands the higher the temperature in these locations. Special case study was Diobu in 1990 map with very high LST but as at 2017 the very high LST increase towards Orogbum, Trans-amadi and Elekahia due to urbanization and industrial activities in Trans-amadi. Trans-amadi is the industrial hub of Port Harcourt which is capable of generating heat that will increase LST.

As one move away from the built-up areas, LST decreases from high to moderately high temperature. As noted in the mangrove wetland, the LST was moderately high to low value. This was due to the regulative ability of wetland to shade water in the wetland from the hot day temperature [44] and from the anthropogenic radiation from urban areas. The very low LST observed in the water body may be due to the ability of water body to absorb heat in the day and release them in the night.

The difference between the mean and minimum temperature of 2017 and 1990 was computed as 1.34°C and 2.45°C. These differences are indication that LST in the study area have increase due to climate change. Using the mean LST as base, the rate of increase of the LST was computed as 0.05°C, which implies that in every year the surface temperature increase by that value.

LST is directly related to vegetation indices. As the LST increases, NDVI and GNDVI value decreases. For example, in 1990 at pixel location with coordinate 276570mE, 531930mN LST was 27.10°C and the NDVI -0.07 was recorded. Similarly, at location with coordinate 281220mE, 529170mN LST was 18.38°C and the NDVI value of 0.27 was recorded. The increase LST and the corresponding decrease in NDVI and GNDVI in 1990 map produced Pearson correlation

coefficient of 0.09 and 0.19 respectively. But in the 2017 map, the Pearson correlation coefficient of LST against NDVI and GNDVI of 0.40 and 0.30 respectively were recorded. These values suggest that there exist week relationship between LST and vegetation indices in the area. However, moderately strong correlation coefficient was observed in 2017 map than that of 1990 map, this was due to continuous increase in urban temperature. Land temperature continuously increase in response to multiple anthropogenic activities taking place in the urban area [45]. While in the water body and vegetation none of these activities occur. The water body serves as reservoir for LST, especially, in the day time and releases it in the night.

4. Conclusion

LST is directly link to climate change. It is never constant but fluctuates from one location to another. LST affected both biotic and abiotic component of the ecosystem. Obtaining spatial distribution of LST is a serious concern to researchers especially in less developed nations like ours. This study was carried out for the purpose of estimating LST of Port Harcourt city using OLI Landsat 8 of 2017 and TM Landsat 5 of 1990 downloaded from its website using path 188 and row 57. The image was clipped in ArcGIS 10.1 software from the clip tool in the raster processing tool in Arc Toolbox. The analysis was based on the converted image from DN to TOA radiance. The study observed mean LST difference between 2017 and 1990 as 1.34°C, indicating an increase in LST in the study area. Also mean difference of the estimated LST from images were close to the values obtained by NIMET in 1990 and 2007. Finally, both NDVI and GNDVI produced positive correlation coefficient with LST. However, a strong correlation was obtained between NDVI and GNDVI in 2017 maps, this may be due to increase in LST of the area. It is therefore recommended that temperature stations should be established at strategic locations in the city for the purpose of observing LST and making such data available for government, researchers and institutions. For further study, LST should be obtained from other remote sensing data on monthly base and compare the results with the in-situ observations at various locations.

Acknowledgement

References

[1]   Rebecca, L. D. and Russell, G. C. (2013). Meeting Environmental Challenges with Remote Sensing Imagery, American Geosciences Institute, 4220 King Street, Alexandria, VA 22302, USA. www.agiweb.org. pp. 44.
[2]   IPCC, (2012). Glossary of terms. In: Managing the Risks of Extreme Events and Disasters to Advance Climate Change Adaptation, [Field, C.B., V. Barros, T.F. Stocker, D. Qin, D.J. Dokken, K.L. Ebi, M.D. Mastrandrea, K.J. Mach, G.-K. Plattner, S.K. Allen, M. Tignor, and P.M. Midgley (eds.)]. A Special Report of Working Groups I and II of the Intergovernmental Panel on Climate Change (IPCC). Cambridge University Press, Cambridge, UK, and New York, NY, USA, pp. 555-564.
[3]   Bhatta, B. (2013). Research Methods in Remote Sensing, Springer Briefs in Earth Sciences, Springer Dordrecht Heidelberg New York London, www. springer.com, pp. 3-5.
[4]   Menzel, P. W. (2006). Remote Sensing Applications with Meteorological Satellites, NOAA Satellite and Information Service University of Wisconsin Madison, WI, pp. 147-162.

[5]   Turner, B. L (2017). Temperature Increase Reduces Global Yields of Major Crops in Four Independent Estimates, PNAS, Vol. 114, No. 35, pp. 9326-9331.

[6]   Stefan, S. and Frank, E. (2014). Future Crop Production Threatened by Extreme Heat, Environ. Res. Lett. Vol. 9, 041001, pp. 1-4.

[7]   Rasul, G., Chaudhry, Q. Z., Mahmood, A. and Hyder, K. W. (2011). Effect of Temperature Rise on Crop Growth & Productivity, Pakistan Journal of Meteorology, Vol. 8, No. 15, pp. 53-62.

[8]   Takeshi, S., Shoichiro, H., Takashi, U., Satoshi, O., Per, M., Ken, K. and Toshiko K. (2016). Temperature Change Affected Groundwater in a Confined Marine Aquifer during Long-term Heating and Cooling, Water Research, Vol. 94, pp. 120-127.

[9]   Makoto, T. (1995). Analysing the Long Term Reduction in Groundwater Temperature due to Pumping, Hydrological Science Journal, Vol. 40, No. 3, pp. 407-421, DOI:10.1080/026266669509491424.

[10]   Alkhaier, F., Flerchinger, G. N. and Su, Z. (2012). Shallow Groundwater Effect on Land Surface Temperature and Surface Energy Balance under Bare Soil Conditions: Modeling and Description, Hydrol. Earth Syst. Sci., Vol. 16, pp. 1817-1831, doi:10.5194/hess-16-1817-2012.

[11]   Susanne, A. B., Peter, B., Gerfried, W. and Philipp B. (2017). Recent Trends of Groundwater Temperatures in Austria, Hydrol. Earth Syst. Sci., pp. 1-16, https://doi.org/10.5194/hess-2017-663.

[12]   Jason, J. G., Randall T. H., and Timothy, R. G. (2009). Effects of Climate Variability and Change on Groundwater Resources of the United States, Facts Sheets, pp. 1-4.

[13]   FAO, (2016). Climate Change and Food Security: Risk and Responses, pp. 1-15.

[14]   Friends of the Earth, (2015). Floods, Climate Change and Flood Defence Investment, See Things Differently, pp. 1-7.

[15]   Forbes, T., and Christina, D. (2014). Heavy Precipitation in the U.S. and the Climate Change Conception, World Resources Institute, Fact Sheet, pp. 1-6.

[16]   UNFCCC, (2007). Climate Change: Impacts, Vulnerabilities and Adaptation in Developing Countries, United Nations Framework Convention on Climate Change, Martin-Luther-King-Strasse 853175 Bonn, Germany, pp. 1-68.

[17]   WHO, (2002). Floods: Climate Change and Adaptation Strategies for Human Health, Report on a WHO Meeting, London, United Kingdom, pp. 1-52.

[18]   Union of Concerned Scientists, (2012). After the Storm: The Hidden Health Risks of Flooding in a Warming World, Climate Change and your Health, Two Brattle Square, Cambridge, MA 02138-3780, pp. 1-24.

[19]   Meijerink, A. M. J. (2007). Remote Sensing Applications to Groundwater, 7, Place de Fontenoy, 75352 Paris 07 SP (France), pp. 44.

[20]   Raunag, J. (2010). Vegetation Indices, FAPAR and Spatial Seasonality Analysis of Crops in Southern Sweden, Master Degree Thesis, Supervised by Dr. Lars Eklundh, Department of Physical Geography and Ecosystem Analysis, Lund University, pp. 5.

[21]   Newfel, M. (2005). Correlation Between NDVI and Surface Temperatures using Landsat ETM Imagery for San Antonio Area, Remote Sensing Project, pp. 1-20.

[22]   Andrew, T., Deirdre, B., and Ryan W. (2002). Coastal Sea Surface Temperature Variability from Landsat Infrared Data, Remote Sensing of Environment, Vol. 81, pp. 262-272.

[23]   Myung-Hee, J., Kwang-Jae, L, Byong-Woon, J., Bong-Kyum, K. and Yun-Won, J. (2001). The Spatial Topographic Analysis of Urban Surface Temperature using Remote Sensing Data and GIS, Paper Presented at the 22nd Asian Conference on Remote Sensing, 5 – 9 November 2001, Singapore, pp. 1-6.

[24]   Hassaballa, A. A. and Matori, A. B. (2011). The use and Evaluation of Split-Window Technigues for NOAA/AVHRR Surface Temperature Extraction over Different Surface Covers: Case Study (Perak Tengah & Manjong) Area Malaysia, International Journal of Civil & Environmental Engineering, Vol. 11, No. 5, pp. 22-27.

[25]   Leonardo, V., Juan, C. P., Luis, M., Cristian, M. and Emilio, J-F. (2010). Comparative Analysis of Split-Window Algorithms for Estimating Soil Temperature, R.C. Suelo Nutr. Vol. 10, No. 1, pp. 35-39.

[26]   National Bureau of Statistics, (2006). Official Gazette (FGP 71/52007/2500 OL24), National and State Provisional Total 2006 Census.

[27]   NIMET, (2011). Nigeria Climate Review Bulletin, pp. 1-40.

[28]   Leadership New Paper, (July 29, 2017). http://leadership.ng/2017/07/29/rage-port-harcourt-creeks/
[29]   ENVI User's Guide, (2004). ENVI Version 4.1, Research System Inc, pp. 14.
[30]   John, C. (2012). PancromaTM Satellite Image Processing Making Satellite BetterTM, Instruction Manual Version 101, pp. 1-399, www.PANCROMA.com.
[31]   USGS, (2017). Product Guide Landsat 4-7 Surface Reflectance (LEDAPS) Product, Version 7.6, pp. 1-35.
[32]   Richard, J. U., and Chima, O. (2016). Analysis of Impact of Land Use/ Land Cover Change in Oguta/ Orashi Watershed, International Journal of Emerging Trends in Engineering and Development, vol. 3, no. 6, pp. 21-34.
[33]   Centre for Biodiversity and Conservation, (2004). Remote Sensing & Geographic Information Systems Facility, American Museum & Natural History, pp.1-16.
[34]   USGS, (2016). Landsat 8 (L8) Data Users Handbook LSDS-1574 Version 2.0, pp. 21-61.
[35]   Anji, M. R. (2008). The TextBook of Remote Sensing and Geographic Information Systems, 3rd Edition, 4-4-309, Giriraj Lane, Sultan Bazar, Hyderabad-500 095-A.P, pp. 93, 191.
[36]   Richards, J. A., and Xiuping, J. (2006). Remote Sensing Digital Image Analysis, 4th Edition, Springer-Verlag Berlin Heidelberg, Germany, pp. 394-395.
[37]   Landsat Technical Guide, (2004). Global Land Cover Facility, University of Maryland Institute for Advanced Computer Studies, Department of Geography, http://ltpwww.gsfc.nasa.gov/IAS/handbook/handbook_toc.html, pp. 1-2.
[38]   Abduwasit, G. (2010). Calculating Surface Temperature using Landsat Thermal Imagery, Macelwane Hall 324 3507 Laclede Ave, St Louis, MO 63103, pp. 1-9.
[39]   Ram, J., Hardik, R., Maharshi, P., Sumit, P., Ajay, P., Vijay, S., Manik, H. K. (2015). Urban Heat Islan Characterization and Isotherm Mapping using Geo-informatics Technology in Ahmedabad City, Gujarat State, India, International Journal of Geosciences, Vol. 6, pp. 274-285.
[40]   Nikolaos G. S., Thomas K. A., Ioannis Z. G., Konstantinos P. (2006). Vegetation Indices: Advances Made in Biomass Estimation and Vegetation Monitoring in the Last 30 Years, Geocarto International, Vol. 21, No. 4, pp. 1-8.
[41]   Rogerson, P. A. (2001). Statistical Methods for Geography, 1st Edition, Sage Publications Ltd. 6 Bonhill Street, London EC2A 4PU, pp. 87-103.
[42]   Singh, Y. K. (2006). Fundamental of Research Methodology and Statistics, New Age International (P) Limited 4835/24, Ansari Road, Daryaganj, New Delhi-110002, pp. 304-308.
[43]   Sundara, K., Bhaskar, P. U., Padmakumar, K. (2012). Estimation of Land Surface Temperature to Study Urban Heat Island Effect using Landsat ETM+ Image, International Journal of Engineering Science and Technology, Vol. 4, No. 2, pp. 771-778.
[44]   Rhode Island Department of Environmental Management, (2008). What's the Scope on Wetlands, Frequently asked Questions about DEM's Freshwater Wetlands Program, RI Department of Environmental Management of Water Resources Groundwater and Wetland Protection Program 235 Promenade St., Providence, RI 02908, pp. 1-53.
[45]   Backluud, P., Schimel D., Janetos, A., Hatfield J., Ryan, M.G., Archer, S. R. and Lettenmaier, D. (2008). The Effects of Climate Change on Agriculture, Land Resources, Water Resources, and Biodiversity in the United States, Synthesis and Assessment Product 4.3 Report by the U.S. Climate Change Science Program and the Subcommittee on Global Change Research, Washington, DC, USA, pp. 13.

*Corresponding author.
E-mail address: jeremiah.uriah@ yahoo.com / andrewabah4real@ gmail.com